



Power Electronic Systems
Laboratory

© 2012 IEEE

Proceedings of the International Conference on Electrical Machines (ICEM 2012), Marseille, France, September 2-5, 2012

Modeling and Comparison of Machine and Converter Losses for PWM and PAM in High-Speed Drives

L. Schwager,
A. Tüysüz,
C. Zwyssig,
J. W. Kolar

This material is published in order to provide access to research results of the Power Electronic Systems Laboratory / D-ITET / ETH Zurich. Internal or personal use of this material is permitted. However, permission to reprint/republish this material for advertising or promotional purposes or for creating new collective works for resale or redistribution must be obtained from the copyright holder. By choosing to view this document, you agree to all provisions of the copyright laws protecting it.



Eidgenössische Technische Hochschule Zürich
Swiss Federal Institute of Technology Zurich

Modeling and Comparison of Machine and Converter Losses for PWM and PAM in High-Speed Drives

Lukas Schwager, Arda Tüysüz, Christof Zwyszig, Johann W. Kolar

Abstract -- The interaction of the machine and the converter is becoming increasingly important, especially for high-speed drives, mainly due to the effect of the converter modulation on the machine losses. The allocation of the losses to different components of the drive system needs to be known in order to choose the ideal machine and modulation match. In this paper, individual models are introduced for calculating the rotor, copper, core and inverter losses, taking the modulation type into account. These models are developed considering two typical high-speed permanent-magnet synchronous motor topologies (slotted and slotless machines) driven by Pulse-Amplitude-Modulation (PAM) and Pulse-Width-Modulation (PWM) converters. The models are applied to two off-the-shelf machines and a converter operating both with PAM and PWM. The test bench used to experimentally verify the models is also described and the model results are compared to the measurements.

The results show that PAM produces a higher overall efficiency for the high-speed machines considered in this work. However, PWM can be used to move the losses from the rotor to the converter at the expense of decreasing the overall drive efficiency. The possible benefits of these results are discussed.

Index Terms-- Electric drives, high-speed, losses, modeling, Permanent-Magnet Synchronous Machines (PMSM), Pulse-Amplitude Modulation (PAM), Pulse Width Modulation (PWM).

I. NOMENCLATURE

$b(x)$	Slot width
f_{PWM}	PWM switching frequency
F, G	Copper loss coefficients
\hat{H}	Peak external field strength
$I_{n,\text{rms}}$	RMS value of the n^{th} current component
J	Current density
m	Space-harmonic number
n	Time-harmonic number
$P_{\text{Cu,p}}$	Proximity effect losses
$P_{\text{Cu,s}}$	Ohmic losses, including skin effect
σ_{Cu}	Conductivity of copper
FE	Finite Element
krpm	1,000 revolutions per minute
PAM	Pulse Amplitude Modulation
PMSM	Permanent-Magnet Synchronous Motor
PWM	Pulse Width Modulation
RMS	root mean square

L. Schwager was with the Power Electronic Systems Laboratory of Swiss Federal Institute of Technology (ETH) Zurich, Switzerland. He is now with ABB Discrete Automation and Motion, Switzerland (e-mail: lukas.schwager@ch.abb.com).

C. Zwyszig is with Celeroton Ltd., Zurich, Switzerland (e-mail: christof.zwyszig@celeroton.com).

A. Tüysüz and J. W. Kolar are with the Power Electronic Systems Laboratory of Swiss Federal Institute of Technology (ETH) Zurich, Switzerland (email: tuysuz@lem.ee.ethz.ch, kolar@lem.ee.ethz.ch).

II. INTRODUCTION

HIGH-SPEED permanent-magnet synchronous motors (PMSMs) with power ratings of a few tens of watts to a few kilowatts and rotational speeds from a few tens of thousands up to a few hundreds of thousands of rpm are employed in micro gas turbines, turbocompressor systems, drills for medical applications, micromachining and optical spindles [1], [2]. The trend towards higher rotational speeds is mainly driven by the need of a higher power density in emerging applications. The main challenges in these drives are the mechanical rotor design and the thermal considerations due to higher losses per surface, considering constant efficiencies [1], [3].

The two typical motor topologies used in high-speed drives are shown in Fig. 1. In both cases a simple, rotation-symmetric rotor structure is used for easy manufacturing and in order to limit the mechanical stresses in the magnet and retaining sleeve. In some cases there is no rotor hub because either a hollow rotor is required (machining spindles) or the center is filled with magnet material (fully cylindrical magnet). Two-pole rotors are commonly used for the lowest possible fundamental electrical frequencies. The stator usually contains distributed three-phase windings and can be of either the slotted or slotless type. Slotless topology, which leads to relatively small machine inductances and low flux densities in the stator core, is widely used for small high-speed drives [1], [4]. Slotted machines are used in machining spindles where higher torque densities are needed.

Motors up to speeds in the area of a few ten thousand rpm, e.g. 50 krpm, are usually driven with Pulse-Width-Modulation (PWM) inverters applying sinusoidal three-phase currents. Due to the high fundamental frequency of the currents, the PWM frequency is increased and/or an AC filter is employed in between the inverter and the motor. At

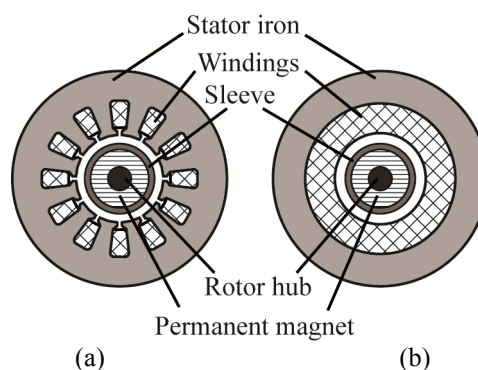


Fig. 1. Conceptual section views of typical slotted (a) and slotless (b) high-speed motors. The rotor hub does not exist in some machines.

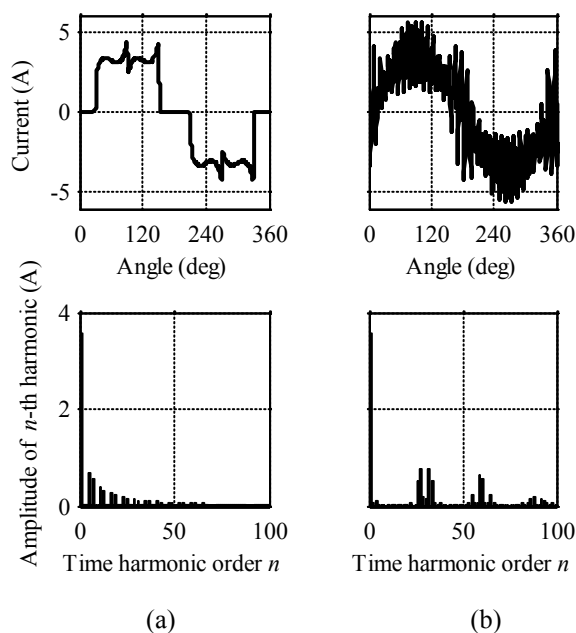


Fig. 2. Typical motor phase current waveforms and current harmonic spectra in the slotless machine for a rotational speed of 100 krpm, PAM modulation (a) and 50 kHz PWM modulation (b).

speeds above 200 krpm Pulse-Amplitude-Modulation (PAM) inverters are suggested in literature [1], [5]. Typical phase current waveforms and their harmonic spectra for both modulation types are depicted in Fig. 2. These phase current waveforms depend strongly on the motor phase inductances.

Ideally, the modulation type and the machine topology should be chosen according to the losses in the machine and the converter. However, this is not a trivial decision as the loss distribution and the total efficiency have a different importance in different applications. In machining spindles for example, the compactness and efficiency of the machine are the key parameters, whereas an oversized, lossy converter is not a major drawback. On the other hand, for compressors in heat pumps or gas turbines the total drive system efficiency is crucial. Furthermore, rotor losses are generally considered to be more problematic due to the limited rotor cooling whereas converter cooling is usually unproblematic. Therefore, the ideal modulation strategy and the ideal motor topology have to be identified according to the application.

In industrial motors the losses are usually specified for sinusoidal currents only. This can be adequate for standard-speed motors where the inverter switching frequency is two or more decades higher than the fundamental electrical frequency and therefore the phase currents are virtually perfectly sinusoidal with a very low current ripple. However, the high-speed motors are driven either with block currents (PAM) or with sinusoidal currents where the current ripple is usually clearly visible (PWM), as layout parasitics, as well as today's practical switches and gate drivers, limit the PWM switching frequency for a given efficiency target. Thus, enhanced loss models are required for high-speed motors taking the current waveform shape into account.

The effect of the inverter supply on the machine losses has been studied in literature. In [6] for example, the dependency of the eddy current losses of a 12.5 MW synchronous machine on the inverter supply is studied. In [7] an experimental efficiency comparison of PAM and PWM controlled brushless DC drives is made; whereas [8]

shows a comparison of PAM and PWM drives with respect to stability issues at high speeds. However, for an appropriate choice of modulation strategy and motor topology for a given application, the influence of the modulation on the individual loss components in motor and inverter should be taken into account, and this is the main goal of this paper.

In this paper loss models which account for the influence of the modulation are implemented to compare the losses of two high-speed PMSMs and converters. Models for different electromagnetic loss components are briefly described. They are then applied to two different off-the-shelf machines driven by PAM and PWM with different switching frequencies. The results are shown and compared to each other. Finally, experimental results are presented to verify the theoretical loss models.

III. LOSS MODELS

A. Rotor loss model

An analytical model is used for calculating the rotor losses. An analytical model has the advantage that it can be quickly evaluated for different modulations, rotational speeds and machines. As the skin depth at the occurring frequencies has the same order of magnitude as the rotor diameter, the eddy current reaction field must be considered. As high-speed machines generally have a small number of poles and a highly conductive rotor sleeve, the model should also account for currents in the sleeve and the rotor curvature.

In [9] a rotor loss model based on the 2D solution of the Maxwell equations considering the effects mentioned above is introduced. An equivalent current sheet is used on the stator bore as the external boundary condition to model the stator windings as equally distributed surface currents on the slot openings. This current sheet can be written as a superposition of combinations of time and space harmonics. Solutions are given for the diffusion equation in the sleeve and the magnet regions as well as for Laplace's equation in the air gap region. Finally, rotor losses are calculated using Poynting's theorem for each combination of time and space harmonics separately.

In this paper the same approach is used, but with different regions and internal boundary conditions. The inner boundary condition is replaced by the claim for continuity on the rotational axis for the rotor construction with a fully cylindrical magnet. Its finite permeability is also considered for the construction with a rotor hub. The machine phase currents are calculated taking the modulation and frequency dependency of the winding inductance into account, and applied to the rotor loss model to calculate the rotor losses.

B. Core loss model

The empirical method of Steinmetz was developed a long time ago and has been widely used for predicting the core losses in inductors, transformers and rotating electrical machines. However, this method is insufficiently accurate when the excitation is nonsinusoidal (as in inductors used in switched power supplies), or if the flux is not only alternating, but also has a rotating component (as in rotating electrical machines). In literature numerous methods are proposed to take those effects into consideration. In [10] the Steinmetz method is modified to account for nonsinusoidal excitation. In [11] the effects of the rotational flux are also taken into account.

In this work, the method presented in [12] is adopted because it takes both nonsinusoidal and rotating flux effects into account, and it needs only the standard loss coefficients which are generally provided by the manufacturers. Furthermore, it calculates the losses in the time domain and it is already implemented in the commercial Finite Element (FE) software package Maxwell from Ansys. The phase currents for PAM and PWM are calculated separately and impressed into the windings of a 2D transient model in the software to calculate the core losses.

C. Copper loss model

The total copper losses in an electrical machine can be calculated as

$$P_{Cu,s} + P_{Cu,p} = \sum_n (I_{n,rms}^2 F + G \frac{\hat{H}^2}{\sigma_{Cu}}), \quad (1)$$

where $P_{Cu,s}$ is the ohmic losses created by the current flowing in the conductor and $P_{Cu,p}$ is the proximity effect losses caused by external fields. Those components of the copper losses are calculated for different frequency components of the current where $I_{n,rms}$ is the rms value of the n^{th} frequency component of the current, \hat{H} is the peak external field strength and σ_{Cu} is the conductivity of copper. The coefficients F and G depend on the winding configuration and the skin depth, and they are calculated according to [13].

As can be seen in (1), the field strength in the winding area is needed to calculate the proximity losses. In the slotless machine topology, this field is the superposition of the permanent-magnet field and the armature field. The magnitude of the armature field is typically much smaller than the magnitude of the permanent-magnet field; however, it contains frequency components higher than the fundamental electrical frequency of the machine; hence it contributes to the losses, especially at higher frequencies. Thus, the proximity losses caused by the rotor and armature fields can be calculated separately and superimposed.

The permanent-magnet field in the slotless machine is calculated analytically according to [14]. A 2D FE model of the machine is used to calculate the armature field.

In the slotted machine topology, the rotor and armature flux is mostly carried in the iron due to its much higher permeability compared to the windings. Therefore, only the stray field is responsible for the proximity losses. The 1-D model shown in Fig. 3 is used to calculate the stray field. If the field is assumed to have only a y-axis component and the permeability of the iron is assumed to be infinite, the field strength can be calculated as

$$\vec{H}(x) = \frac{1}{b(x)} \int_0^x \vec{J}(x') dx', \quad (2)$$

where J is the current density.

D. Converter loss model

The power electronics converter consists of a three-phase six-step inverter only (PWM) or a three-phase inverter and an additional buck converter (PAM). The buck converter is modeled with a constant efficiency of 98.5% as its losses in the semiconductors and the passives do not depend on the shape of the phase current, and therefore the machine type. The inverter comprises six IGBTs, and the inverter losses can be split into switching and conduction losses. The conduction losses are calculated with the IGBT and diode

forward voltages and on resistances from datasheets and the according average and rms currents of the phase current waveforms. The turn-on and turn-off energies of the IGBTs and diodes have been measured in a separate setup for a range of current and voltage operating points. For the switching loss calculation this data is interpolated at the operating points according to the phase current waveforms and motor voltages. Finally, the switching energies are multiplied by the switching frequency and summed up with the conduction losses for the total inverter losses. In the case of PAM 1.5% of the inverter input power is added for the total converter losses to account for the buck converter losses.

IV. MODEL RESULTS

A. Investigated machines and converters

The loss models described earlier are applied to one slotted and one slotless machine, both driven with PAM and PWM. Both the slotless and the slotted machines have one pole pair and they are designed for the nominal speed of 200 000 rpm and nominal torque of 30 mNm. The slotless machine has skewed Faulhaber-type air-gap windings with 54 turns per phase. The stator is made of amorphous iron. The rotor of the slotless machine is made of a one piece

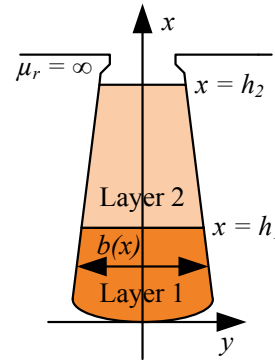


Fig. 3. 1-D model of the stray field in the slotted machine topology. A 2-layer winding is assumed.

diametrically magnetized magnet, contained by a grade 5 titanium sleeve. The slotted machine has two layer windings inserted into 18 slots. The number of turns per phase is 57. The stator core is made of thin non-oriented, fully-processed 0.2 mm electrical steel laminations. The rotor of the slotted machine is similar to that of the slotless machine, with an additional rotor hub made of magnetic steel 1.4104 at its center. The flux linkage, phase inductance and resistances are 5.61 mVs, 65 μ H and 0.49 Ω for the slotless machine; 5.94 mVs, 300 μ H and 1.14 Ω for the slotted machine. The stators of the two machines can be seen in Fig. 4.

The converter used in this work is the CC-230-3000 from Celeroton. The converter consists of a buck converter, connected to the DC side of a 3-phase 6-switch voltage source inverter [14]. The buck converter is bypassed in PWM operation. The inverter switches are International Rectifier IRGP50B60PD1s.

B. Rotor losses

The calculation of the rotor losses for different time and space harmonics of the machine current reveals that the

impact of the space harmonics is very small. The rotor losses, for example for PAM and a speed of 100 krpm caused by the fundamental and the higher order space harmonics are 4.29 W and 118 μ W for the slotless machine and 6.34 W and 3.88 mW for the slotted machine. The large effective air gap of the machines is considered to be the main reason for these results.

Fig. 5 and Fig. 6 show the rotor losses produced by the time harmonics normalized to the square of the amplitude of the exciting current harmonic for the two machines. It can be seen that the increase of losses flattens for higher time harmonics. This is due to the eddy current reaction field which prevents the field from entering the conducting region. This effect is significantly stronger for the slotted machine than for the slotless machine. This effect lowers the losses of PWM with respect to PAM as the current harmonics are of a higher order but generally smaller amplitude for PWM. This leads to lower rotor losses at higher PWM frequencies.

The effects of different time and space harmonic combinations can be seen in Fig. 7.

C. Core losses

As described earlier, using the instantaneous core loss calculation method in [12] allows for the comparison of time behaviours of the core losses under different modulation methods. Although the instantaneous core losses look different for PAM and PWM, the average core loss depends only slightly on the modulation. The average core losses under no-load for a speed of 100 krpm, PAM and

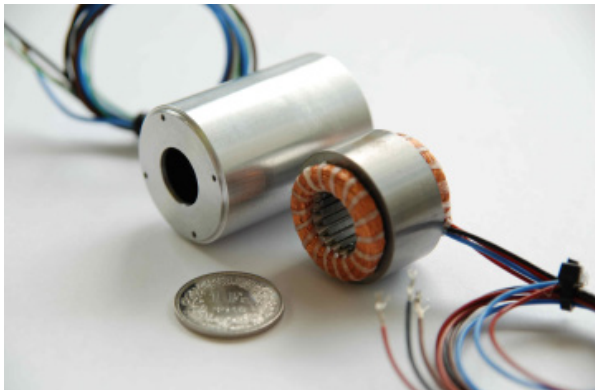


Fig. 4. Stators of the slotless (left) and the slotted (right) machines.

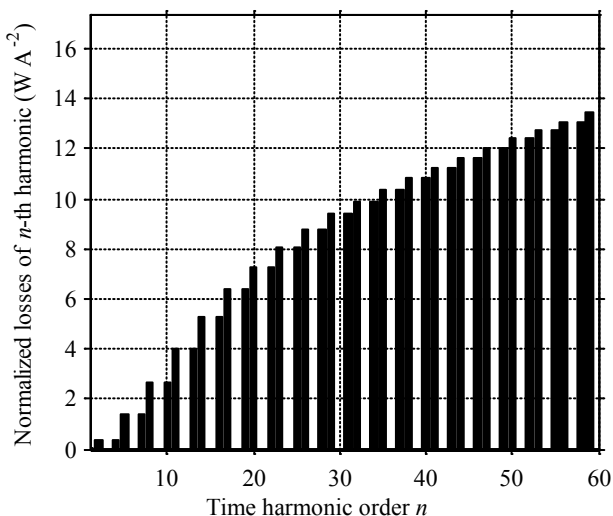


Fig. 5. Losses of time harmonics for the slotless machine and a rotational speed of 100 krpm.

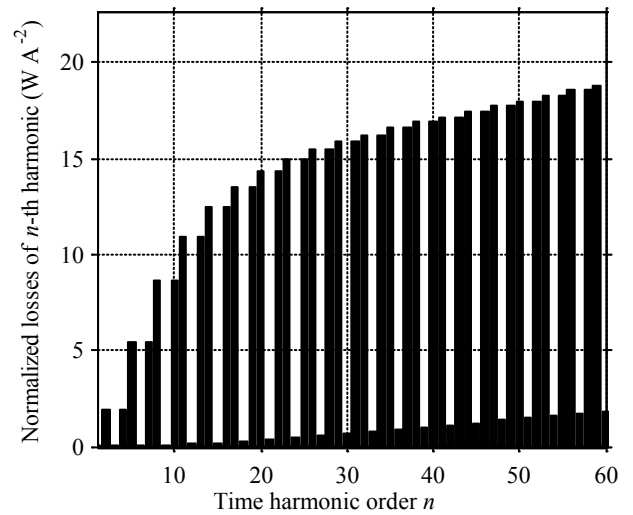


Fig. 6. Losses of time harmonics for the slotted machine and a rotational speed of 100 krpm.

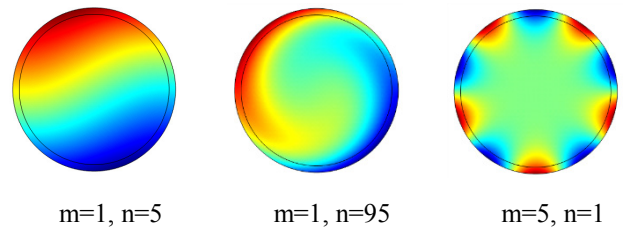


Fig. 7. The effects of different time (n) and space (m) harmonics on the rotor losses. Rotor eddy currents are plotted. (red) into the direction of the page, (blue) out of the direction of the page.

50 kHz PWM are 674 mW, 735 mW and 1.02 W for the slotless machine and 6.7 W, 8.2 W and 7.15 W for the slotted machine.

D. Copper losses

The windings of both the slotless and the slotted machines considered in this work are made of litz wire, with strand diameters of 71 μ m and 170 μ m, respectively. Thus, the calculated F coefficient in (1) is practically equal to the DC resistance of the windings up to frequencies around 50 kHz. This means that the first part of (1) does not depend on the modulation type.

The proximity losses are calculated for a typical fundamental frequency of 1.67 kHz (100 krpm) and a switching frequency of 50 kHz. Table 1 shows the different components of the proximity losses. It can be seen that proximity losses produce a rather small amount of the total losses; however they can become important when the high frequency components of the drive current also have high amplitudes.

TABLE 1
PROXIMITY LOSS COMPONENTS

	Slotless machine	Slotted machine
Rotor flux (1.67 kHz)	453.46 mW	
Armature reaction (1.67 kHz)	55.195 μ W/A ²	
Armature reaction (50 kHz)	49.674 mW/A ²	
Stray field (1.67 kHz)		191.46 μ W/A ²
Stray field (50 kHz)		172.18 mW/A ²

E. Total drive system losses

The comparison of all the loss components for the slotless machine under PAM and PWM operations are shown in Fig. 8 for a speed of 100 krpm. The iron losses are very small with respect to the total losses, and hardly visible in

the plot. This is due to the low-loss amorphous core material. Iron losses depend only slightly on the modulation type, since the armature reaction field is much smaller than the permanent-magnet field.

The copper losses make a large contribution to the losses but also show a weak dependence on modulation. This is due to the fact that neither skin nor proximity effect losses have a significant effect at the frequencies occurring. The fundamental component of the current is mainly responsible for the copper losses, and it is kept the same for all modulations in order to maintain the same torque.

It is mainly the rotor losses out of the machine losses which depend on the modulation. The amplitude of the current ripple decreases but its frequency increases with increasing PWM frequency. One would expect that this would lead to constant rotor losses, with these two effects cancelling each other out. However, the eddy current reaction prevents the armature reaction field's penetration into the entire rotor. This results in decreasing rotor losses with increasing PWM frequencies.

The PWM frequency for the slotless machine considered needs to be increased beyond 200 kHz to achieve lower machine losses than for PAM, at the speed of 100 krpm.

While the machine losses decrease for higher PWM frequencies, the converter losses increase due to increasing switching losses. In respect of the total losses, the optimum PWM frequency is 90 kHz but the total losses in this case are still more than twice as high as for PAM.

The machine losses for the slotless machine are plotted for a speed range between 50 krpm to 200 krpm in Fig. 9.

Results of the loss models for the slotted machine are shown in Fig. 10 for a speed of 100 krpm. Iron and copper losses for the slotted machine are larger compared to the slotless machine. Similar to the slotless machine, iron and copper losses depend to a very small extent on the modulation type whereas converter and rotor losses change significantly with modulation. The machine losses for a PWM frequency greater than 35 kHz are smaller than for PAM. The machine losses for a switching frequency of 50 kHz are 5 W less compared to PAM whereas the converter losses are higher by 7.9 W.

The machine losses for the slotted machine are plotted for a speed range between 50 krpm to 200 krpm in Fig. 11.

V. EXPERIMENTAL RESULTS

The test set-up in Fig. 12 is built to verify the loss models by experiments. The converter under test drives the machine under test at a constant speed. The load machine dissipates the mechanical power in a load resistor connected through a passive rectifier. As the load power and the mechanical losses are constant for a given speed, the influence of a different modulation can be easily measured by measuring the input power to the machine and the converter.

In Fig. 13, the measured and calculated difference of the machine losses under PWM and PAM operations are given for different PWM frequencies. The comparison of calculated and measured inverter losses are shown in Fig. 14.

The mismatch of PAM inverter losses is within the expected accuracy of ± 6 W for that particular measurement setup. The significant mismatch of the machine losses for the slotless machine is assumed to be as a result of asymmetrical currents due to the PAM which cannot control the phase currents individually. The model, however, assumes symmetrical phase currents and therefore shows

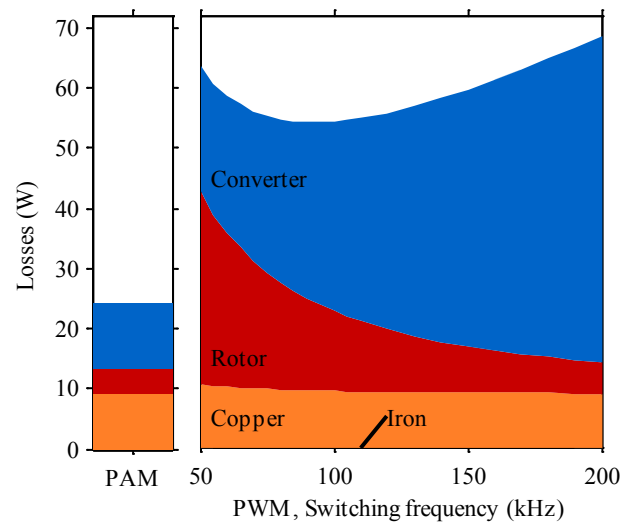


Fig. 8. Comparison of model results for the slotless machine and a rotational speed of 100 krpm.

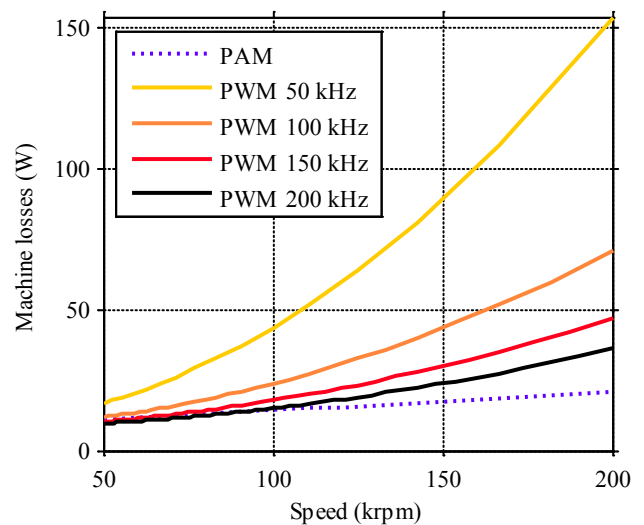


Fig. 9. Machine losses of the slotless machine over rotational speed.

smaller losses than in measurement for PAM. This results in a higher difference of losses under PWM with respect to losses under PAM in model, showing up in Fig. 13. The quantification of this modeling error and possible remedies are the subject of undergoing research.

Apart from that, it can be concluded that the loss models can accurately predict the effects of different modulations on the machine losses as well as the inverter losses.

VI. CONCLUSION

Interaction of the motor and the inverter is becoming increasingly important, especially at higher rotational speeds. Comparison of different inverters and modulation types for a given drive application can be found in literature. There are also studies on the effects of the inverter supply on the machine losses. However, the selection of the ideal machine, inverter topology and modulation type is still open. One of the main reasons for this is the different level of importance of various loss components in a drive system. In spindle applications, for example, the machine needs to be very compact, limiting the cooling options in the machine. The converter, on the other hand, can generally be placed in locations where the space limits are not critical and better cooling options are available. In such applications, higher converter losses can

be tolerated in order to decrease the machine losses. On the other hand, for compressors the overall efficiency of the drive system is required to be as high as possible.

In this work, individual models for calculating the rotor, copper, stator core and inverter losses are given. These models are developed considering two typical high-speed PMSM topologies (slotted and slotless machines) and two typical converter types (PWM and PAM). The models are applied to two off-the-shelf machines driven both by PAM and PWM inverters.

The results show that for the slotless machine used in this work PAM gives much higher efficiency, both in the machine and the converter, for speeds between 50 krpm and 200 krpm.

The overall drive system losses for the slotted machine under PAM and PWM are much closer to each other, with PAM still producing less overall losses at 100 krpm. However, it is clearly shown that by using PWM with an appropriate switching frequency, the losses can be moved from the rotor to the converter, with the expense of slightly decreasing overall efficiency. This result can be used in applications where the rotor losses are more important than the overall efficiency, as described above.

Finally, a test setup is built to measure the losses for different machines, under different modulations. Experimental results verify the validity of the models.

Future work includes the optimization (both geometry and materials) of the machines using the models introduced in this paper. Furthermore, both the PWM and PAM modulations can be further optimized, e.g. for lowest rotor losses.

VII. ACKNOWLEDGMENT

The authors gratefully acknowledge the contributions of ATE Antriebstechnik und Entwicklungs GmbH, who provided the slotted machine used in this work.

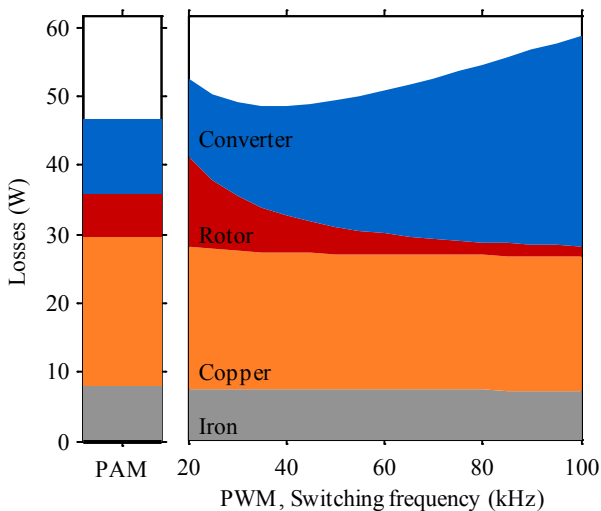


Fig. 10. Comparison of model results for the slotted machine and a rotational speed of 100 krpm.

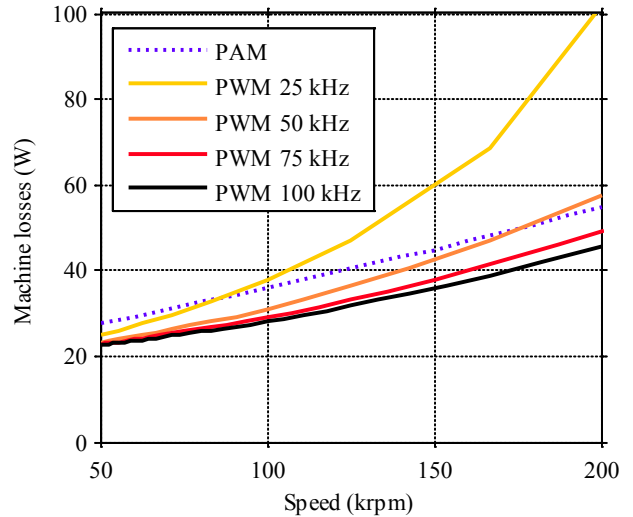


Fig. 11. Machine losses of the slotted machine over rotational speed.

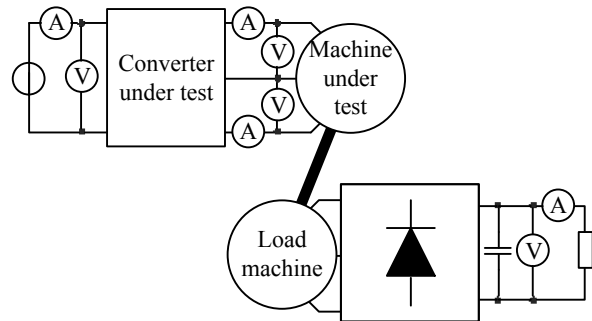


Fig. 12. The test bench used to verify the models experimentally.

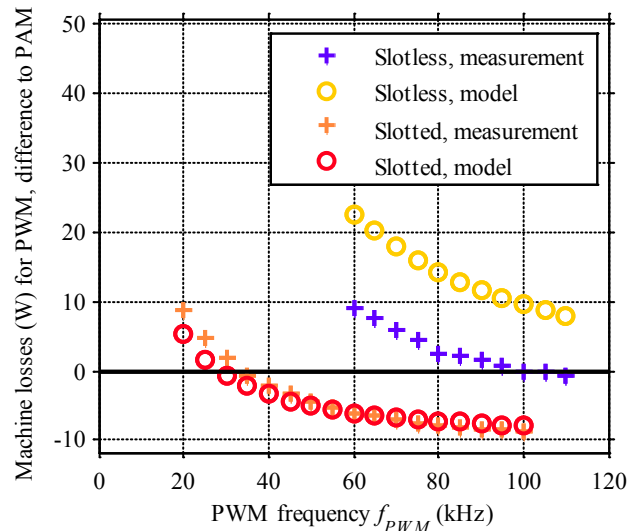


Fig. 13. Deviation of measured as well as modeled machine losses for both machines and a rotational speed of 100 krpm for PWM with respect to PAM.

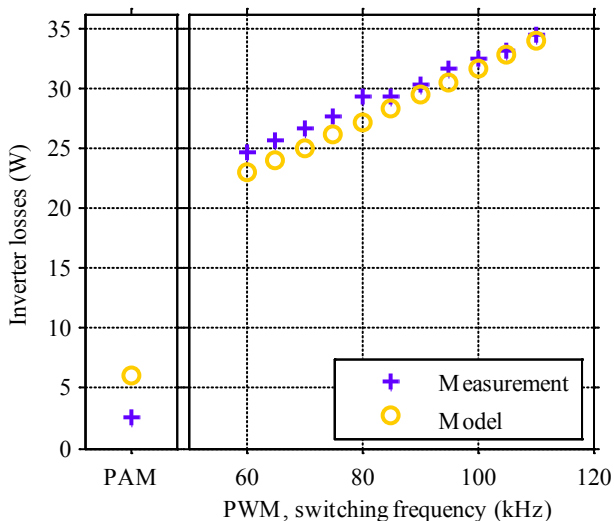


Fig. 14. Calculated and measured inverter losses for the slotless machine at 100 krpm.

VIII. REFERENCES

- [1] C. Zwyssig, J. W. Kolar, and S. D. Round, "Megaspeed Drive Systems: Pushing Beyond 1 Million r/min," *IEEE/ASME Trans. On Mech.*, vol. 14, no. 5, pp. 564-574, Oct. 2009.
- [2] M. A. Rahman, A. Chiba, and T. Fukao, "Super high speed electrical machines—Summary," *Proc. IEEE Power Eng. Soc. General Meeting*, vol. 2, pp. 1272–1275, Jun. 2004.
- [3] A. Binder and T. Schneider, "High-speed inverter-fed AC drives," *Int. Aegean Conf. Electr. Mach. Power Electron.*, Sep. 2007.
- [4] A. Looser, T. Baumgartner, C. Zwyssig, and J. W. Kolar, "Analysis and measurement of 3D torque and forces for permanent magnet motors with slotless windings," *IEEE Proc. Of. Energy Conv. Cong. and Exp.*, pp.3792-3797, Sep. 2010.
- [5] K. Taniguchi and A. Okumura, "A PAM inverter system for vector control of induction motor," *Proc. PCC Conf.*, pp. 478-483, 1993.
- [6] P. Rasilo, and A. Arkkio, A, "Modeling the effect of inverter supply on eddy-current losses in synchronous machines," *Int. Symp. on Power Elec. Elec. Drives Automation and Motion*, pp. 861-865, Jun. 2010.
- [7] L. Yen-Shin, L. Ko-Yen, T. Jing-Hong, C. Yen-Chang, and H. Tse Liang, "Efficiency comparison of PWM-controlled and PAM controlled sensorless BLDCM drives for refrigerator applications," *IEEE Conf. Rec. of the 42nd IAS Ann. Meeting Ind. Appl. Conf.*, pp. 268-273, Sep. 2007.
- [8] K. H. Kim and M. J. Youn, "Performance comparison of PWM inverter and variable DC link inverter schemes for high-speed sensorless control of BLDC motor," *Electronics Letters*, Vol. 38, pp. 1294-1295, 2002.
- [9] Z.Q. Zhu, K. Ng, N. Schofield and D. Howe, "Improved analytical modelling of rotor eddy current loss in brushless machines equipped with surface mounted permanent magnets," *IEE Proc.-Electr. Power Appl.*, Vol. 151, No. 6, Nov. 2004
- [10] J. Reinert, A. Brockmeyer, and R.W. De Doncker, "Calculation of losses in ferro- and ferrimagnetic materials based on the modified Steinmetz equation," *IEEE Trans. on Ind. Appl.*, vol.37, no.4, pp.1055-1061, Jul.-Aug. 2001.
- [11] L. Ma, M. Sanada, S. Morimoto, and Y. Takeda, "Iron loss prediction considering the rotational field and flux density harmonics in IPMSM and SynRM," *IEE Proc. Electric Power Appl.*, vol. 150, no. 6, pp. 747-751, Nov. 2003.
- [12] D. Lin, P. Zhou, W. N. Fu, Z. Badics, and Z. J. Cendes, "A dynamic core loss model for soft ferromagnetic and power ferrite materials in transient finite element analysis," *IEEE Trans. on Magn.*, vol.40, no.2, pp. 1318-1321, Mar. 2004.
- [13] J. A. Ferreira, *Electromagnetic modeling of power electronic converters*. Norwell, USA: Kluwert Academic Publishers, 1989.
- [14] C. Zwyssig, "An ultra-high-speed electrical drive system. PhD thesis, ETH Zurich, 2008.

IX. BIOGRAPHIES

Lukas Schwager received the M.Sc. degree in electrical engineering from the Swiss Federal Institute of Technology (ETH) Zurich, Zurich, Switzerland, in 2011. During his studies, he focused on power electronics, electrical machines and control systems and did his master thesis at

Celeroton, Zurich, Switzerland, a spin-off company in the area of high-speed electrical drive systems.

He has been working as a R&D engineer for Medium Voltage Drives in ABB Discrete Automation and Motion, Switzerland since January 2012.

Arda Tüysüz received his B.Sc. degree in Electrical Engineering from Istanbul Technical University in Turkey in 2006 and M. Sc. degree from RWTH Aachen University in Germany in 2009.

In his M.Sc. thesis he worked on the full-speed range self-sensing of ultra-high-speed electrical machines. Since June 2009, he is with the Power Electronic Systems Laboratory of Swiss Federal Institute of Technology (ETH) Zurich as a Ph.D. student. His Ph.D. research focuses on novel electrical machine topologies for high-speed drives and self-sensing control of high-speed electrical machines.

Christof Zwyssig received the M.Sc. and Ph.D. degrees in electrical engineering from the Swiss Federal Institute of Technology Zurich, Switzerland, in 2004 and 2008, respectively. He studied power electronics, machines, and magnetic bearings and was engaged in research on high-speed electrical drive systems and their power electronics. Since January 2009, he has been with Celeroton AG, Zurich, a spin-off company in the area of high-speed electrical drives, of which he is a cofounder.

Johann W. Kolar received the M.Sc. and Ph.D. degrees from the University of Technology Vienna, Vienna, Austria.

He has been an independent international consultant in close collaboration with Vienna University of Technology in the fields of power electronics, industrial electronics, and high-performance drives since 1984. He proposed numerous novel pulse-width-modulation converter topologies, as well as modulation and control concepts, e.g., the Vienna rectifier and the three-phase alternating-current (ac)-ac sparse matrix converter. On February 1, 2001, he was appointed Professor and Head of the Power Electronic Systems Laboratory, Swiss Federal Institute of Technology (ETH) Zurich, Zurich, Switzerland. He is the author or co-author of more than 350 scientific papers published in international journals and conference proceedings. He is the holder of more than 75 patents. His current research focuses on ac-ac and ac-direct-current converter topologies with low effects on the mains, e.g., for power supply of data centers, more electric aircraft, and distributed renewable energy systems. Furthermore, the main areas of his research are the realization of ultra-compact and ultra-efficient converter modules employing latest power semiconductor technology (SiC and GaN), novel concepts for cooling and electromagnetic interference filtering, multi-domain/multi-scale modeling/simulation and multi-objective optimization, physical model-based lifetime prediction, pulsed power, and ultrahigh-speed and bearingless motors.

Dr. Kolar is a member of the Institute of Electrical Engineers of Japan (IEEJ). He is a member of the international steering and technical program committees of numerous international conferences in the field (e.g., Director of the Power Quality Branch of the International Conference on Power Conversion and Intelligent Motion). He is the founding Chairman of the IEEE Power Electronics Society (PELS) Austria and Switzerland Chapters and the Chairman of the Education Chapter of the European Power Electronics and Drives Association. From 1997 to 2000, he served as an Associate Editor of the IEEE TRANSACTIONS ON INDUSTRIAL ELECTRONICS. Since 2001, he has been an Associate Editor of the IEEE TRANSACTIONS ON POWER ELECTRONICS. Since 2002, he has also been an Associate Editor of the Journal of Power Electronics of the Korean Institute of Power Electronics and a member of the Editorial Advisory Board of the IEEJ Transactions on Electrical and Electronic Engineering. He was a recipient of the Best Transactions Paper Award from the IEEE Industrial Electronics Society (IES) in 2005, the Best Paper Award at the International Conference on Power Electronics in 2007, the 1st Prize Paper Award from the IEEE Industry Applications Society Industrial Power Converter Committee in 2008, the IEEE Industrial Electronics Conference Best Paper Award from the IES Power Electronics Technical Committee in 2009, the 2009 PELS Transaction Prize Paper Award, and the 2010 Best Paper Award of the IEEE/ASME Transactions on Mechatronics. He also received an Erskine Fellowship from the University of Canterbury, Christchurch, New Zealand, in 2003. He initiated and/or is the founder/cofounder of four spin-off companies targeting ultrahigh-speed drives, multidomain/multilevel simulation, ultra-compact/ultra-efficient converter systems, as well as pulsed-power and electronic energy processing. In 2006, the European Power Supplies Manufacturers Association awarded the Power Electronics Systems Laboratory of ETH Zurich as the leading academic research institution in Power Electronics in Europe.